The ultrafast photodissociation of $Fe(CO)_5$ in the gas phase

L. Bañares,[a] T. Baumert, M. Bergt, B. Kiefer, and G. Gerber
Physikalisches Institut, Universität Würzburg, D-97074 Würzburg, Germany

(Received 18 August 1997; accepted 17 November 1997)

The photodissociation dynamics of $Fe(CO)_5$ in a molecular beam have been investigated with femtosecond time resolution. In single pulse experiments, the parent ion $Fe(CO)_5^+$ and all the fragment ions $Fe(CO)_n^+$, $n=0-4$ could be observed in linear and reflectron time-of-flight (TOF) spectrometers. Ladder switching is suppressed by the use of femtosecond laser pulses. The TOF spectra show that the fragmentation patterns strongly depend on the laser wavelength, the laser intensity, and the laser pulse duration. Femtosecond pump–probe experiments were performed for the parent and every fragment molecule. We present a photodissociation model for the neutral $Fe(CO)_5$. After the absorption of two 400 nm photons, $Fe(CO)_5$ looses four CO ligands in about 100 fs. The subsequent dissociation of the fragment Fe(CO) takes place on a longer time scale of about 230 fs. The measured transient ionization spectra of the $Fe(CO)_n$, $n=2-4$ fragments represent within the proposed model the fingerprints of the evolution of the $[Fe(CO)_5]^{\ddagger}$ transition state on the way to dissociation. We also report on the observation of a metastable ionic fragmentation mechanism. © *1998 American Institute of Physics.* [S0021-9606(98)00808-3]

I. INTRODUCTION

The photochemistry of metal carbonyls is of great importance in the understanding of interesting properties of these compounds.[1,2] Metal carbonyls are widely used as photocatalysts in many organic reactions.[3–5] It has been shown[3–5] that highly reactive unsaturated species coming from the photolysis of M–CO bonds, where M is a transition metal atom, are responsible for this catalytic activity. In a completely different context, the full photodissociation of these molecules has been applied in microelectronics as a means of growing thin ultrapure metal films onto surfaces.[6] The basic understanding of the fragmentation mechanism by which these complex molecules loose one or several CO ligands after the absorption of a photon with sufficient energy is of great interest.

The photodissociation of monometal carbonyls in solution is simple. After laser excitation, the molecule looses only one CO ligand.[1–3] Collisional relaxation and cage effects with the solvent molecules avoid the loss of additional CO ligands because the excess internal energy of the fragments is rapidly dissipated to the surrounding medium. The picture is quite different in the gas phase if, in addition, collisionless conditions are guaranteed. In this case, several ligands can leave the complex after absorption of a single photon with sufficient energy. The proportion of unsaturated fragments will then depend on the photolysis wavelength and laser intensity, since multiphoton processes can also be involved. Indeed, this is a basic difference between the photochemistry of metal carbonyls, and organometallics in general, and that of most of the small organic and inorganic molecules, where only one bond is usually broken upon absorption of one photon. Whether the loss of ligands by the metal atom after one photon or multiphoton absorption happens sequentially or in a concerted fashion has been the subject of controversy.[7]

$Fe(CO)_5$ is a prototype molecule whose study can provide a good understanding of the photodissociation mechanism of metal carbonyls. For this molecule, plenty of theoretical information is available about its molecular and electronic structure.[8–15] In addition, *ab initio* calculations with different degrees of sophistication have been performed in the last few years in order to obtain accurate values of the first and subsequent dissociation energies of the Fe–CO bonds, not only for the neutral $Fe(CO)_5$,[15–20] but also for the ion molecule $Fe(CO)_5^+$.[21] The theoretical results have been compared with experimental data obtained by photodetachment of mass-selected beams of carbonyl anions $Fe(CO)_n^-$ [22] by pulsed laser pyrolysis of $Fe(CO)_5$ (Ref. 23) and by other techniques.[24–27]

Time-resolved experiments using ultrafast laser pulses have been performed with metal carbonyls and organometallics in solution (see, e.g., Refs. 28–35). The first ultrafast gas phase study was reported by Angel *et al.*,[36] who measured the vibrational dynamics of $Co(CO)_3NO$. Zewail and co-workers[37] recently reported the first photodissociation experiments in the gas phase. They studied the ultrafast fragmentation dynamics of $Mn_2(CO)_{10}$. In this cornerstone experiment, the metal–metal and metal–ligand bond cleavage dynamics, occurring on a time scale of hundreds of femtoseconds, could clearly be distinguished. In a very recent experiment by Harris and co-workers,[38] the dissociation dynamics of $M(CO)_6$ (M=Cr, W, Mo) in solution has been studied by femtosecond IR spectroscopy. It was concluded that the formation of the metal pentacarbonyl product after UV photolysis of the parent molecule occurs in less than 240 fs, the resolution of their apparatus.

As stated by Grant and co-workers in 1983, ''no tech-

[a]Alexander von Humboldt Foundation research fellow. Permanent address: Departamento de Química Física, Facultad de Química, Universidad Complutense, 28040 Madrid, Spain.

nique applied thus far has been fast enough to measure an actual primary dissociation rate'' for $Fe(CO)_5$.[39] The application of femtosecond lasers to study the photodissociation of this molecule and metal carbonyls in the gas phase is very timely. In a previous publication,[40] we reported the first experiments where the photodissociation dynamics of $Fe(CO)_5$ in a molecular beam was studied with femtosecond time resolution. The parent molecule and all the fragments were detected after femtosecond laser excitation in a linear time-of-flight (TOF) spectrometer. Transient ionization spectra of the parent molecule and of every fragment were measured by using the femtosecond pump–probe technique. From the results obtained in that study, it was concluded that the photodissociation of $Fe(CO)_5$ up to Fe(CO) occurs in about 100 fs. The subsequent dissociation of Fe(CO) into Fe+CO occurred on a longer time scale. A mechanism was proposed to explain these observations. The present paper is a full account of the results obtained on the gas phase photodissociation of $Fe(CO)_5$ from our laboratory. We report additional experiments on the femtosecond laser intensity and wavelength dependence of linear and reflectron TOF spectra, where even doubly charged species have been observed, and we report on additional femtosecond pump–probe experiments. The results confirm the previously proposed mechanism for the photofragmentation of $Fe(CO)_5$ in the gas phase.

This paper is organized as follows: In Sec. II we give an overview of the available spectroscopic informations for the metal carbonyl $Fe(CO)_5$. The experimental setup for single pulse and pump–probe measurements is described in Sec. III and the obtained results are presented in Sec. IV. In Sec. V we report laser-induced metastable decays of $Fe(CO)_5$ observed with our reflectron time-of-flight spectrometer.

II. SPECTROSCOPY AND PHOTOCHEMISTRY OF $Fe(CO)_5$

$Fe(CO)_5$ is a trigonal bipyramid which belongs to the D_{3h} point symmetry group (see Fig. 1). The energetics of the neutral and ion molecules are presented in Fig. 1. The information contained in Fig. 1 is a combination of the available experimental and theoretical data. The absorption spectrum was measured in the liquid phase by Dartiguenave *et al.*[41] in 1969, and later in the gas phase by Kotzian *et al.*[12] In both cases, the spectrum (shown schematically in Fig. 1) is rather structureless. It exhibits a strong band centered at about 50 000 cm^{-1} with a shoulder at 41 600 cm^{-1} (indicated by arrows in Fig. 1). These two bands have been assigned to metal to ligand charge transfer (MLCT) $d \rightarrow \pi^*$ transitions.[12] The absorption starts at about 25 000 cm^{-1} and shows two weak shoulders at 30 300 and 35 700 cm^{-1}, which have been assigned to ligand field (LF) $d \rightarrow d$ transitions.[12] The assignments are supported by theoretical studies by several groups.[10–12] These works showed that in spite of the large number of electronic states involved, the metal–carbonyl near-ultraviolet spectrum is determined exclusively by MLCT transitions and that the lowest lying singlet excitations in $Fe(CO)_5$ are predicted to be LF transitions.[12] The most recent experimental value for the first ionization potential of $Fe(CO)_5$ was reported by Norwood *et al.*[26] (7.897 ± 0.025 eV; 63 689 cm^{-1}), and is very close to the one of

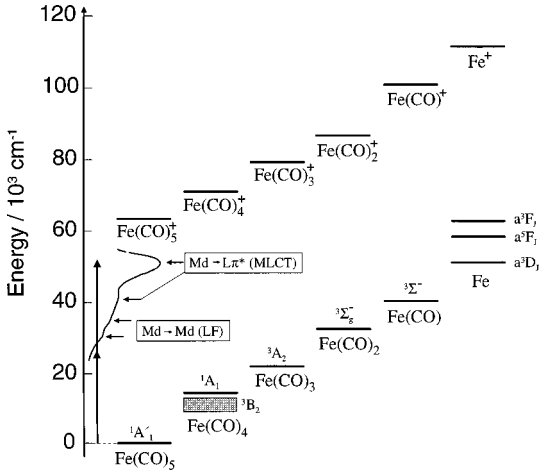

FIG. 1. Energetics of $Fe(CO)_5$. The information shown is a compilation of experimental and theoretical data of the neutral and ionic molecules. The gas phase absorption spectrum (Ref. 12) is shown schematically and the assignments to LF and MLCT transitions are indicated by horizontal arrows. The shaded area corresponds to the range of calculated (Refs. 16 and 18) energies for the electronic ground state of $Fe(CO)_4$. The vertical arrows indicate the two photon excitation at 400 nm discussed in the text.

atomic Fe (7.870 eV).[42] The vacuum-ultraviolet (VUV) spectrum of $Fe(CO)_5$ was also measured recently[14] and, based on *ab initio* calculations, two series of Rydberg states were assigned in the spectral ranges between 49 600 and 61 800 cm^{-1} and between 64 100 and 71 800 cm^{-1}.

Many experimental studies have been reported on the photodissociation of $Fe(CO)_5$ in the gas phase using nanosecond lasers in combination with other techniques. The pioneering works by Karny *et al.*[43] and Trainor and Mani[44] showed the emission of electronically excited Fe atoms produced after laser excitation of $Fe(CO)_5$. Duncan *et al.*[45] reported multiphoton ionization (MPI) experiments where Fe^+ was the dominant ion in the mass spectra. Engelking[46] observed atomic Fe transition lines in the MPI spectra of $Fe(CO)_5$. Yardley and co-workers[47,48] were the first to measure the distribution of $Fe(CO)_{4-2}$ fragments at different one-photon excitation excimer-laser wavelengths (193, 248, and 352 nm). By using a chemical trapping technique consisting of the photolysis of gaseous mixtures of $Fe(CO)_5$ and PF_3 in a cell, they measured the quantitative yields of the products $Fe(CO)_{5-n}(PF_3)_n$, $n=0-3$. The authors proposed a photodissociation process in which the CO ligands are lost sequentially. The experimental results were in agreement with their (RRKM) calculations in which only one vibrational mode was coupled to the reaction coordinate (i.e., the motion of the CO ligand with respect to the metal atom). According to these calculations, about 65% of the available energy was retained by nascent $Fe(CO)_4$ fragment as vibrational and/or electronic excitation. Grant and co-workers,[39] using MPI to monitor the CO product after photolysis of the parent molecule in the region 290–310 nm, reported an inverted vibrational energy distribution in this fragment. The inverted distribution implied a nonstatistical energy release in the photofragmentation process. The authors obtained estimates of less than 0.6 ps for the lifetime of $Fe(CO)_5$ excited

states in the 275–280 nm excitation region and of less than 2 ps in the 300–310 nm region.

Weitz and co-workers[49,50] reported transient infrared absorption spectra of the coordinatively unsaturated species generated after excimer-laser photolysis of $Fe(CO)_5$. The absorption features were assigned to the $Fe(CO)_n$ fragments via comparison with results obtained in matrix isolation studies.[51–54] Waller, Hepburn, and co-workers[55,56] measured the rovibrational and translational distributions of the CO product by VUV laser-induced fluorescence (LIF) in a molecular beam. Vernon and co-workers[57,58] recorded mass spectra containing the parent and all the fragment ions produced by excimer laser photolysis at selected scattering laboratory angles using a crossed laser-molecular beam apparatus. The neutral photoproducts were ionized by electron bombardment and mass selected in a TOF spectrometer. All these studies[49,50,55–58] were in agreement with a sequential mechanism found for the (excimer laser) photodissociation of $Fe(CO)_5$. In all cases and even in the work of Yardley and co-workers,[47,48] the ultimate photodissociation product was $Fe(CO)_2$. It was argued by Waller *et al.*[55,56] that the energy retained by the $Fe(CO)_2$ fragment, after $Fe(CO)_5$ absorption of one 193 nm photon and a sequence of three CO ligands cleavages, is not sufficient to further dissociate into $Fe(CO)+CO$. In the work of Vernon and co-workers[57,58] it was concluded that, if high photon fluxes are provided, a second photon can be absorbed by the $Fe(CO)_2$ fragment to loose the two remaining CO ligands sequentially.[57,58]

Photolysis laser wavelengths different than the ones provided by excimer lasers have been also used to study the ground and electronic excited states of Fe [produced after multiphoton dissociation of $Fe(CO)_5$] via MPI[59–61] and photoelectron (PE)[60,61] spectroscopies and LIF.[62–64]

Within this experimental scenario, several theoretical calculations have suggested mechanisms and estimates of the time scales involved in the photodissociation reaction. Daniel *et al.*[10] carried out *ab initio* calculations of the potential energy surfaces (PESs) which connect the ground and lowest excited states of $Fe(CO)_5$ with the ground and excited states of the $Fe(CO)_4$ product. For the $Fe(CO)_5 \rightarrow Fe(CO)_4+CO$ photodissociation reaction these authors proposed a nonadiabatic crossing between the optically allowed lowest singlet excited state and a triplet state which correlates with the ground triplet state of the $Fe(CO)_4$ product. This mechanism was used later by Weitz and co-workers[49,50] and Waller *et al.*[55,56] to explain their experimental results. Recent theoretical studies were carried out by Daniel, Manz, and co-workers on Fe and Co carbonyl hydrides,[65–68] where the PESs involved were calculated by *ab initio* methods and the dynamics were simulated by wave packet propagation. These theoretical studies have shown that the time scale for the cleavage of the metal–CO bond from the lowest electronically excited state is about 100 fs.

As already mentioned in Sec. I, it has been a subject of controversy whether the loss of ligands by the metal atom after laser excitation occurs stepwise or in a concerted way.[7] The main difference between a stepwise and a concerted process is whether or not stable intermediate species are formed. A stepwise reaction involves two or more kinetic steps via detectable intermediates. Houston and co-workers[69,70] defined concertedness when the lifetime of the intermediates is shorter than its rotational period. A more stringent definition is given by Zewail and co-workers,[71] who used the time of the vibrational period for distinction. Typical vibrational periods for the Fe–CO bonds are 80–100 fs.[15]

III. EXPERIMENT

The experimental setup has been described in detail elsewhere.[72] Only the details relevant to the present experiments will be given here. A home-built Ti:sapphire oscillator yields pulsed femtosecond laser radiation centered at 800 nm with a typical duration of 30 fs. The femtosecond pulses are amplified in a modified commercial regenerative amplifier pumped by a 1 kHz Nd:YLF laser. The output of this system, after appropriate recompression, consists of pulses of 80 fs and of about 1 mJ energy per pulse at a wavelength of 800 nm. After second-harmonic generation (SHG), the 400 and 800 nm lasers are separated by means of a dichroic mirror into two beams. The pump laser pulses (400 nm) are delayed with respect to the probe laser pulses (800 nm) using a computer controlled Michelson-type interferometer. Both laser beams, appropriately attenuated, are recombined using a dichroic mirror and focused into the molecular beam chamber (see Fig. 2). The full width at half-maximum (FWHM) of the cross correlation of pump and probe pulses was determined to be 120 fs by sum frequency mixing in a 0.1 mm BBO crystal. A one color pump–probe scheme has also been applied in the present work. The 400 nm laser beam generated by SHG is splitted in pump and probe beams of the same intensity. The probe is time delayed with respect to the pump and both are recombined again and focused onto the molecular beam.

In some of the experiments a home-built colliding pulse mode-locked (CPM) ring dye laser system was used as the source of femtosecond pulses. The output of this laser system consists of amplified pulses of 100 fs centered at a wavelength of 620 nm with a pulse energy of 40 μJ. Nanosecond

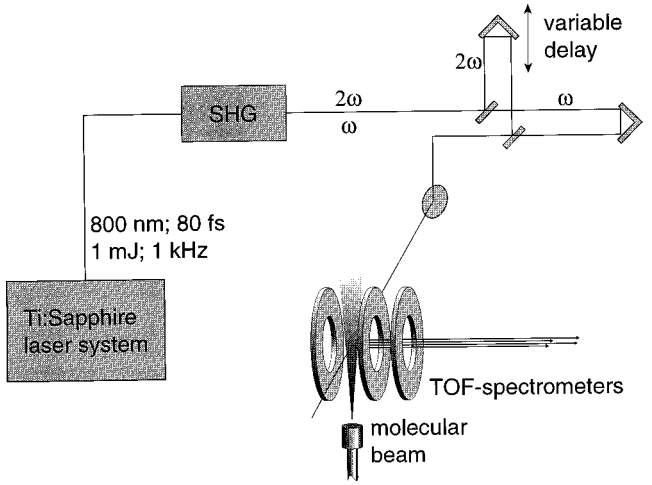

FIG. 2. Experimental setup showing the Ti:sapphire femtosecond laser system used in the present experiments. The ions produced by femtosecond laser excitation in a molecular beam are detected in linear and reflectron TOF spectrometers.

laser pulses are provided by a N_2 laser with pulsed laser radiation at 337 nm, 3 ns pulse duration, and a peak energy of 1 mJ per pulse.

For the reported experiments different molecular beam machines were used. The machines consist of two differentially pumped chambers, one of them containing the $Fe(CO)_5$ source and the other one either a linear time-of-flight (LITOF) spectrometer or a reflectron time-of-flight (RETOF) spectrometer with a field-free drift length of 122 cm. The typical mass resolution of the LITOF is $m/\Delta m = 150$ and $m/\Delta m = 2000$ for the RETOF. The $Fe(CO)_5$ sample, used without further purification (98%; Strem Chemicals), is taken directly from the cylinder at room temperature (vapor pressure of $\approx 3\times 10^3$ Pa) and expanded through a nozzle of 50 μm. In the molecular beam machines, the signal from the MCP detector is recorded by a 500 MHz digital oscilloscope.

The transient ionization spectra, i.e., the ion signal for a given mass in the TOF spectra dependent upon the time delay between the pump and the probe lasers, are measured by means of boxcar integrators. Alternatively, a computer program was developed for data acquisition from the averaged trace of the oscilloscope at selected mass peaks of the spectra. These traces were recorded as a function of the pump–probe time delay. In both cases, the transients were averaged to obtain sufficiently good signal-to-noise ratios. In most of the experiments, the polarization of the pump laser (400 nm) was parallel to the TOF spectrometer axis, whereas the probe laser polarization was perpendicular to it. Changing the polarization of the pump and probe lasers did not affect the measured transients.

The transients were fitted using a nonlinear least-square method based on a Marquardt–Levenberg algorithm where the corresponding molecular response function (single or multiple exponential with rise and decay components) was convoluted with a Gaussian whose FWHM was taken from the measured cross-correlation of the laser pulses (FWHM$\approx$120 fs).

IV. TIME-OF-FLIGHT SPECTRA

A. Nanosecond versus femtosecond excitation

Nanosecond and femtosecond laser pulses at different wavelengths were used in the present experiments to excite $Fe(CO)_5$. When using nanosecond laser pulses, the only mass peak observed in the TOF spectra at different laser intensities was Fe^+, the ion fragment. No evidence of larger fragment ions $Fe(CO)_n$, $n=1-4$, or the parent ion $Fe(CO)_5$ was obtained which is in agreement with earlier nanosecond laser studies.[60–62] Figure 3(a) shows a typical LITOF spectrum obtained from the photolysis of $Fe(CO)_5$ with nanosecond N_2 laser pulses at intensities of about 10^{10} W cm^{-2}. $Fe(CO)_5$ absorbs a photon already within the rising edge of the laser pulse and the molecule dissociates. The resulting fragment molecules absorb additional photons of the same laser pulse and can dissociate further. This process, called ladder switching,[73] leads to the ultimate photodissociation products Fe and CO which absorb more photons and ionize. We do not detect CO^+ ions, because on the one hand the ionization potential (IP) of CO (14.014 eV)[42] is nearly twice

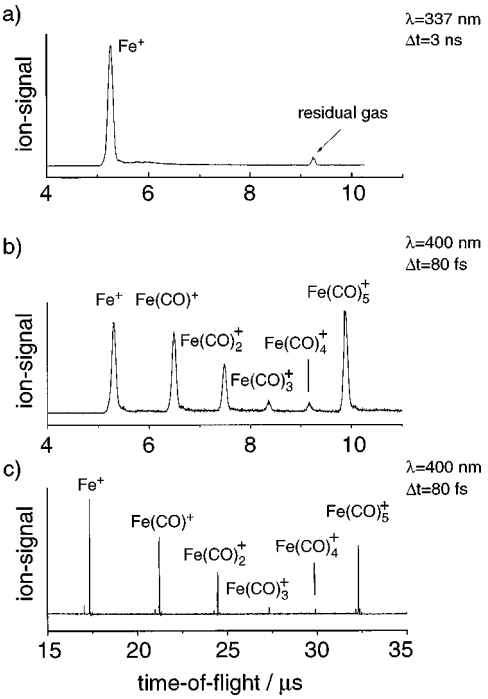

FIG. 3. TOF spectra obtained after irradiation of $Fe(CO)_5$ with nanosecond (a) and femtosecond [(b), (c)] laser pulses measured in a linear [(a), (b)] and a high resolution reflectron TOF spectrometer. Note that the parent molecule and all the fragment ions appear in the TOF spectra when femtosecond laser pulses are used, whereas only Fe^+ is observed in the nanosecond laser TOF spectrum.

of that of Fe (7.870 eV).[42] On the other hand, the produced Fe atomic fragment is highly excited as reported by Karny *et al.*[43] and Engelking[46] and therefore less photons are needed to ionize it. This experiment already shows that the photodissociation of $Fe(CO)_5$ is ultrafast and one has to use ultrashort laser pulses to examine the fragmentation dynamics of this molecule in detail. A similar behavior has been observed in MPI experiments on sodium clusters.[74]

The use of femtosecond laser pulses leads to a completely different picture. Figures 3(b) and 3(c) show the LITOF and RETOF mass spectra obtained with femtosecond laser pulses of 400 nm (intensity of $\approx 10^{13}$ W cm^{-2}). In contrast to the nanosecond laser TOF spectrum, the parent ion, all the fragment ions and CO^+ appear in the mass spectra. Even doubly charged species could be observed at laser intensities higher than $\approx 5\times 10^{13}$ W cm^{-2} [see Figs. 6(a) and 6(b)]. $Fe(CO)^{++}$ and $Fe(CO)_3^{++}$ are clearly resolved but Fe^{++}, $Fe(CO)_2^{++}$, and $Fe(CO)_4^{++}$ appear exactly at the same arrival time in the TOF spectra as the CO^+, Fe^+, and $Fe(CO)^+$ ions, as the time-of-flight t is proportional to $\sqrt{m/q}$. Thus, these three peaks show contributions from singly and doubly charged fragment ions. Figure 4 depicts details of a RETOF spectrum for the $Fe(CO)_5^+$, Fe^+, and CO^+/Fe^{++} mass peaks. The higher resolution obtained with the RETOF spectrometer allows the observation of the different isotopes of the singly and doubly charged species. Every iron containing fragment shows the same isotopic pattern, due to the natural abundance of the different isotopes of ^{54,56,57}Fe, ^{12,13}C, and ^{16,18}O. They all show a prominent peak (relative intensity 1.000) at mass m, a peak at $m-2$, and a

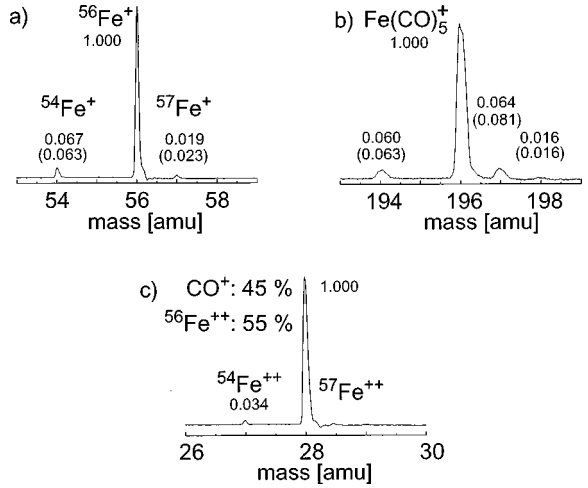

FIG. 4. Details of a reflectron TOF spectrum obtained from $Fe(CO)_5$ using 800 nm femtosecond laser pulses ($\approx 10^{14}$ W cm^{-2}) for the (a) Fe^+, (b) $Fe(CO)_5^+$, and (c) Fe^{++}/CO^+ mass peaks. The largest peak in each case, corresponding to the most abundant ^{56}Fe isotope, has been normalized to one. The relative intensities of the other isotopes, ^{54}Fe and ^{57}Fe, are labeled in the corresponding peaks (the natural abundance is indicated between parenthesis). In the case of the Fe^{++}/CO^+ mass peak, the relative intensity of both ions, appearing exactly at the same time of arrival in the mass spectrometer, has been obtained (Fe^{++}, 55% and CO^+, 45%).

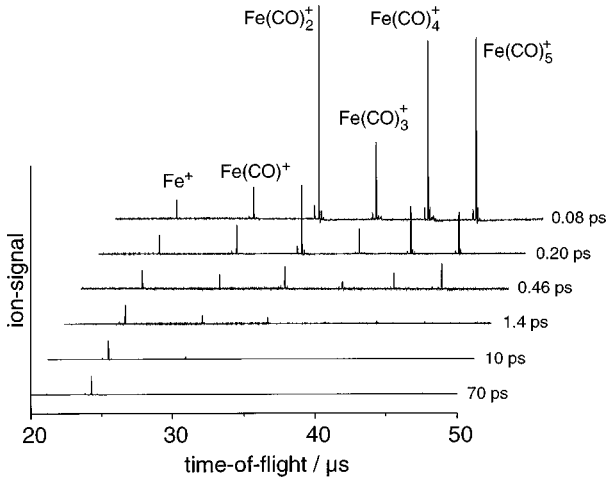

FIG. 5. Reflectron TOF spectra obtained from $Fe(CO)_5$ after excitation using 800 nm variable laser pulse widths between 80 fs up to 70 ps. All the traces have been normalized to have the same Fe^+ mass peak intensity. The parent molecule and all the fragments are observed when laser pulse widths between 80 fs up to 1.4 ps are used. For laser pulse widths of more than 70 ps, only Fe^+ is observed in the spectra.

peak at $m+1$ with less intensity. The relative intensities vary with the number of CO ligands and the estimated intensities due to the natural abundances are indicated in Fig. 4 in paranthesis. In the case of doubly charged species, the isotopic pattern changes to $m-1$, m $m+\frac{1}{2}$, as shown in Fig. 4(c) for the peak at $m=28$ amu/e, which is a combination of doubly charged Fe and singly charged CO. By determination of the relative intensity of the peak at 27 amu/e, we can estimate the contribution of Fe^{++} to 55%.

From the experiments shown in Fig. 3, it is concluded that the duration of the laser pulses plays an important role in the fragmentation dynamics of $Fe(CO)_5$. In order to investigate the dependence of the $Fe(CO)_5$ fragmentation pattern on the laser pulse duration, an experiment was performed where the temporal width of the pulses produced by the femtosecond Ti:sapphire laser system at 800 nm was varied between 80 fs and 100 ps by modifying the alignment of the compressor. The results of these investigations are depicted in Fig. 5. All the RETOF spectra shown in Fig. 5 have been normalized to the same Fe^+ fragment intensity. The small satellite peaks observed for the parent and every fragment ion correspond to the different isotopes of Fe and C atoms. All the fragment ions and the parent ion are observed using laser pulses with durations up to 1.4 ps, although the relative intensities of the different mass peaks change. At a laser pulse duration of 10 ps, the only fragments observed are $Fe(CO)^+$ and Fe^+, and with more than 70 ps laser pulse duration, the only mass peak observed is Fe^+. Experiments with different attenuations of the laser beam show that this effect is mainly due to the laser pulse duration. These results indicate an ultrafast fragmentation dynamics. A time scale of 70 ps is long enough for the fragmentation of the parent molecule. The fragments are then able to absorb additional photons within the laser pulse duration to undergo further fragmentation and ionization. Only if very short laser pulses are used (80 fs), multiphoton ionization will precede fragmentation.

B. Femtosecond TOF spectra

The LITOF spectra obtained using the 400 and 800 nm femtosecond lasers at different intensities are shown in Fig. 6. The parent molecule, all the fragments, and, for the highest laser intensities applied ($\approx 10^{14}$ W cm^{-2} generated for both wavelengths) also doubly charged species were observed for both wavelengths. The ion fragment distribution clearly depends on both the wavelength and the intensity of the laser. For the lowest laser intensities applied ($\approx 10^{11}$ W cm^{-2}), the only mass peak observed is that of the parent ion. Note that at least six photons of 800 nm are needed to ionize $Fe(CO)_5$. As the laser intensity is increased, the various fragments start to appear. Only at higher intensities, the CO fragment is observed due to the fact that at least 16 photons of 800 nm are needed to produce CO^+ via dissociative ionization (ten photons of 800 nm are necessary to ionize CO). Note that these high femtosecond laser intensities of about 10^{14}–10^{15} W cm^{-2} can also lead to field ionization as discussed in detail in a previous publication.[75]

There are interesting differences between the two sets of TOF spectra shown in Fig. 6. In the 800 nm series, $Fe(CO)_2^+$ is the most favored ion fragment from middle to high laser intensities (with the only exception of very high laser intensities where Fe^+ is the most prominent ion). In contrast, the Fe^+ fragment is the dominant ion in the 400 nm experiments. The peak intensities of the $Fe(CO)_4^+$ and $Fe(CO)_3^+$ fragments are similar to that of the parent molecule for 800 nm excitation, whereas for 400 nm excitation the peak intensities of these two fragments are very small. A possible explanation why the $Fe(CO)_2^+$ is favored with 800 nm laser excitation is that the available energy after absorption of seven photons of 800 nm is sufficient for the parent ion to undergo fragmentation up to $Fe(CO)_2^+$ (see Fig. 1). This intermediate state

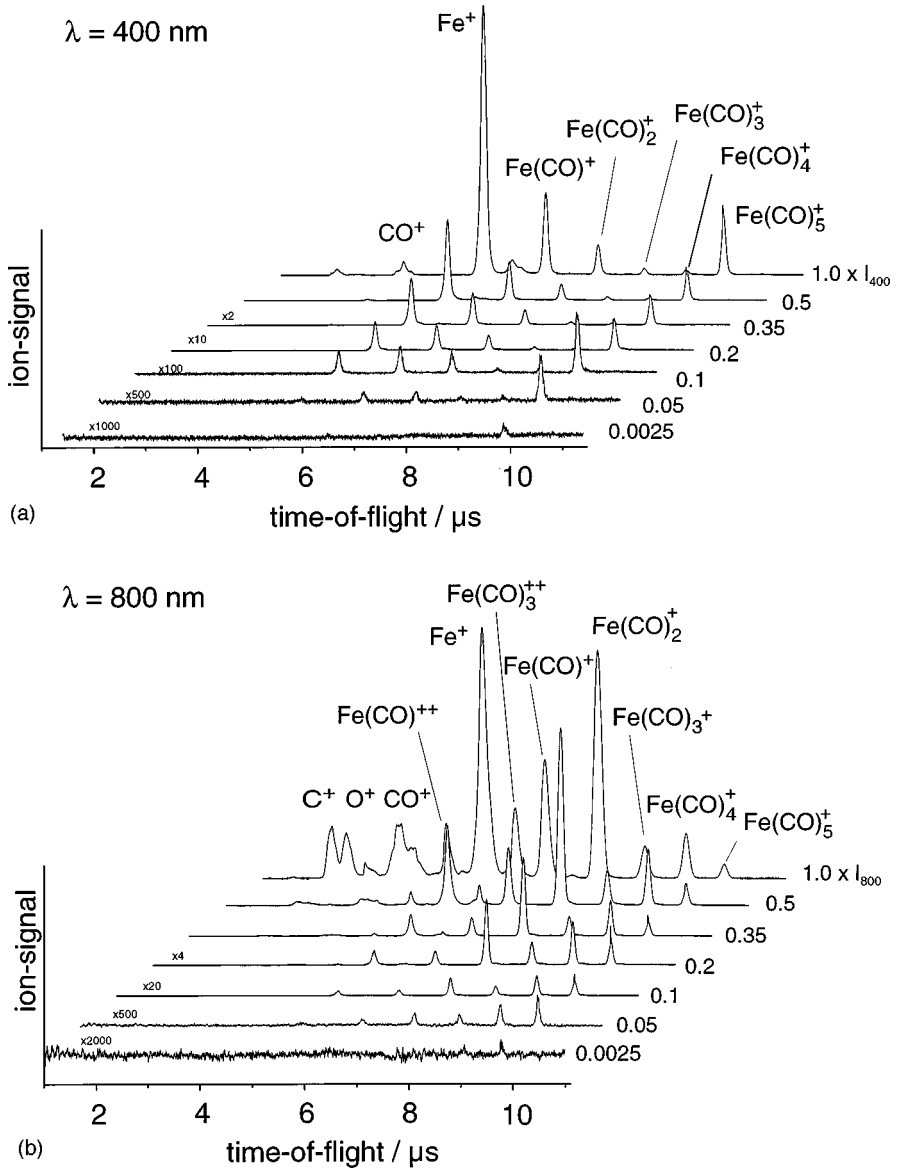

FIG. 6. Linear TOF spectra from $Fe(CO)_5$ using different femtosecond laser wavelengths and intensities: (a) $\lambda = 400$ nm, (b) $\lambda = 800$ nm. $I_{800} \approx 10^{14}$ W cm^{-2} and $I_{400} \approx 10^{14}$ W cm^{-2}. At the highest laser intensities applied doubly charged fragment ions are observed in the spectra.

excitation is not possible with the 400 nm laser. The different fragmentation patterns observed experimentally are most likely due to the fact that more fragmentation channels are opened by using 800 nm radiation compared to 400 nm excitation. The TOF results indicate that the femtosecond fragmentation pattern obtained for $Fe(CO)_5$ strongly depends on the laser wavelength. The results also indicate that multiphoton fragmentation of the parent molecule is occurring most likely via dissociative ionization, i.e., ionization precedes fragmentation. After the absorption of six or more photons of 800 nm (three or more photons of 400 nm), the parent molecule will, most probably, first ionize and later undergo fragmentation to an extent that will depend on the number of photons absorbed, i.e., on the available excess energy.

To further assess the femtosecond laser wavelength dependence of the $Fe(CO)_5$ fragmentation pattern, Fig. 7 shows the series of LITOF spectra obtained from the 620 nm femtosecond laser at different intensities. This series of TOF spectra were measured using ion extraction conditions different from those used for the measurements in Fig. 6. The small peaks observed to the left of the parent and every fragment mass peaks are the species which corresponds with the ^{54}Fe isotope. At sufficient laser intensities doubly charged species are also observed. Under these conditions, the $Fe(CO)_2^+$, $Fe(CO)^+$, and Fe^+ ion fragment peak intensities are larger than the parent $Fe(CO)_5^+$ and the largest fragment ions $Fe(CO)_4^+$ and $Fe(CO)_3^+$, even at the lowest laser intensities applied in the 620 nm experiment ($\approx 10^{13}$ W cm^{-2}). The most prominent ion in the series is always Fe^+, followed by $Fe(CO)^+$ and $Fe(CO)_2^+$. The parent ion and the $Fe(CO)_3$ and $Fe(CO)_4$ fragment ions show similar intensities. Note that even for the lowest laser intensities applied, it is not possible to produce the parent ion alone. In a similar experiment Grotemeyer and co-workers[76,77] excited $Fe(CO)_5$ with 500 fs laser pulses at 260 nm and observed the parent ion

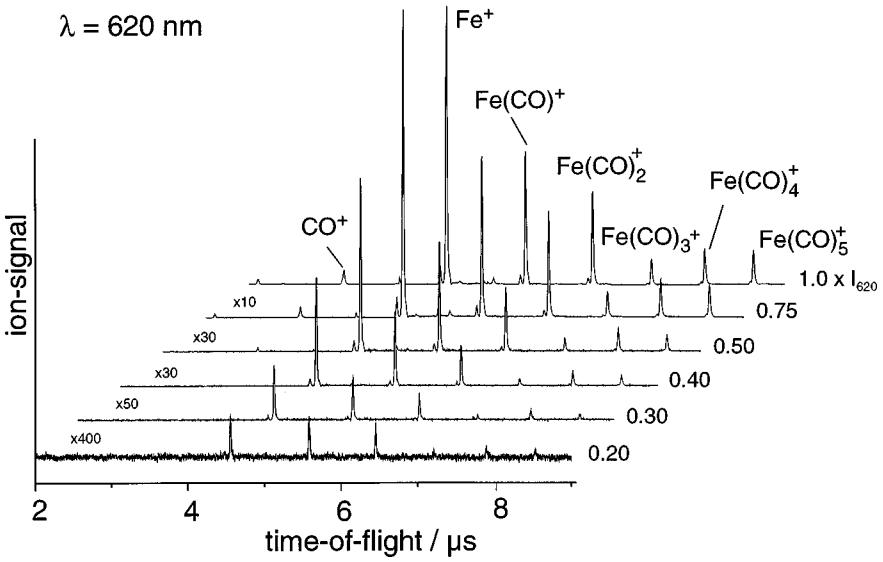

FIG. 7. Linear TOF spectra from $Fe(CO)_5$ obtained using 620 nm femtosecond laser pulses at different laser intensities. $I_{620} \approx 10^{14}$ W cm^{-2}.

and all the fragment ions. However, in this study they were not able to produce the parent ion alone.

In summary, the TOF results shown in Figs. 5–7 indicate that the femtosecond fragmentation pattern obtained for $Fe(CO)_5$ strongly depends on the laser wavelength and the laser pulse duration. The results indicate that for ultrashort laser pulses, multiphoton fragmentation of the parent molecule is most likely via dissociative ionization, i.e., femtosecond ionization precedes fragmentation. On the basis of the data presented up to here, we are unable to give an estimate for the time scale on which photodissociation occurs. The application of femtosecond pump–probe techniques should give further insights into the ultrafast photodissociation dynamics of $Fe(CO)_5$. The femtosecond time scale is the ultimate time scale for real-time observations of nuclear motion in molecules. See, e.g., Refs. 72 and 78–81.

V. TRANSIENT IONIZATION SPECTRA

Transient ionization spectra are recorded by employing the femtosecond pump–probe technique. One and two color pump–probe experiments were performed using the fundamental wavelength (800 nm) and the second harmonic (400 nm) of the Ti:sapphire femtosecond laser system.

A. 400/800 nm transients

Figure 8 shows the measured two color transient ionization spectra of the parent molecule and of every fragment. For positive delay times, the 400 nm laser was the pump and the 800 nm was the probe. All the transients were measured with attenuated pump and probe laser beams, where conditions similar to the bottom traces in Figs. 6(a) and 6(b) were established. Under these experimental conditions, the observed dynamics has to occur in the neutral molecule where the probe laser induces the ionization. In the 400 nm pump laser experiments, the absorption of two photons leads to an excitation of the strong band centered at around 50 000 cm^{-1}—Ref. 12 (see Fig. 1). The very weak absorption observed at 25 000 cm^{-1} (Ref. 12) and the fact that more 800 nm probe photons are necessary to reach the ionization continuum support the two photon excitation at 400 nm.

As can be seen in Fig. 8, the transients of the parent molecule, the $Fe(CO)_4$, and the $Fe(CO)_3$ fragments show some ion signal before time zero, i.e., when pump (400 nm) and probe (800 nm) lasers interchange their role. In the case of the parent molecule, the asymptotic ion signal at negative delay times is even larger than at positive delay times. This effect strongly depends on the intensity of the pump and probe lasers. Several experiments were performed at different attenuations of both lasers to further investigate this effect. As the intensity of the lasers was decreased, the ion signal for negative delay times was reduced to the same level as the ion signal for positive delay times and the structure of the transients for negative delay times disappeared. The same happened to the ionization transients of the fragments. Figure 9 shows the transient ionization spectra measured with the

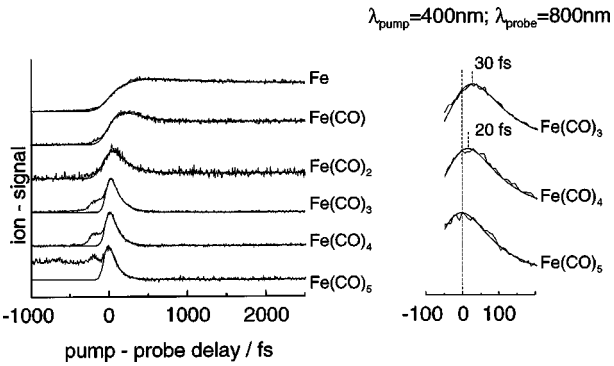

FIG. 8. Two color (400 nm/800 nm) femtosecond transient ionization spectra of the parent molecule and of the fragments. The transients were measured with attenuated pump and probe lasers beams, where conditions similar to the bottom traces in Figs. 6(a) and 6(b) were established. The solid lines represent the fits to the data based on exponential rise and decay constants. The inset shows the expanded transients around time delay zero for the parent molecule and the $Fe(CO)_4$ and $Fe(CO)_3$ fragments. The observed time shifts of the transients are indicated.

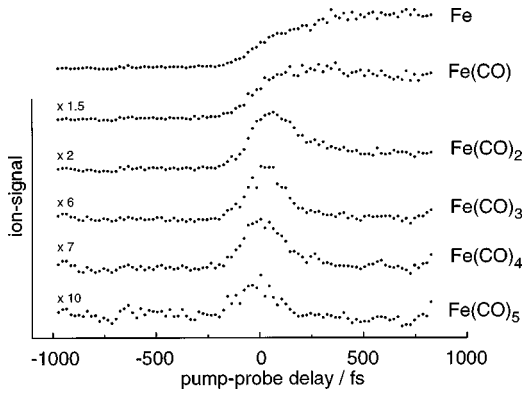

FIG. 9. As in Fig. 8 but taken with the RETOF for the lowest laser intensities of the pump and probe lasers at which pump–probe signal is observed. In this case, clean rise and decay components were observed for the parent molecule and the fragments.

RETOF for the lowest laser intensity. Clean rise and decay curves of the ionization signals are observed. The data of Fig. 8 show the richness of the dynamics of this system. For the 800 nm pump laser, there are at least two possible excitations of the neutral molecule: a three photon excitation to a LF state or a four photon excitation to a MLCT state. The latter excitation is similar to the one obtained after absorption of two photons of 400 nm. It is possible that part of the signal observed for negative and positive delay times in Fig. 8 corresponds to the same process. In addition to that a further process is initiated which shows no time dependence on the measured time scale.

In the following, that part of the transients is analyzed for which the pump excitation is at 400 nm and the subsequent dynamics is probed by 800 nm photons. All the measured transients (Figs. 8 and 9) were fitted to single or multiple exponentials with rise and decay times taking into account the cross correlation of the pump and probe laser pulses. The results of the fits for the parent molecule and all the fragments are shown in Fig. 8 as solid lines. The rise and decay time constants obtained are listed in Table I. The transient of the parent mass and the transients of the fragments $Fe(CO)_4$ and $Fe(CO)_3$ were fitted to single exponentials with decay times of 100 ± 5, 105 ± 5, and 115 ± 5 fs, respectively. In addition, the analysis of the $Fe(CO)_4$ and $Fe(CO)_3$ ionization transients showed time shifts with respect to the maximum of the signal in the $Fe(CO)_5$ ionization transient of 20 ± 5 and 30 ± 5 fs, respectively. The $Fe(CO)_2$ ionization transient was fitted to a single exponential with a decay time of 150 ± 20 fs to an asymptotic level which is constant up to the longest measured delay time of 100 ps. In this case, the time shift with respect to the maximum of the $Fe(CO)_5$ transient was about 60 fs. The Fe(CO) ionization transient showed a slower rise than that of the cross correlation of the pump and probe laser, and was fitted with a rise time of 120 ± 20 fs and a longer decay time of 230 ± 20 fs. For the Fe(CO) ionization transient the asymptotic level was considerably higher than for the $Fe(CO)_2$ [the ratio of the decay amplitude to the amplitude of the time independent contribution was ≈10 for the $Fe(CO)_2$ transient compared to ≈2 for the Fe(CO)]. The transient of the atomic Fe fragment was fitted to a single-exponential rise with a time constant of 260 ± 20 fs and a longer decay time of 490 ± 50 fs with a ratio of amplitudes (decay to time independent contribution) of ≈1.

TABLE I. Rise and decay times from the fits of the transients for the different masses (parent molecule and fragments).

Species	τ_{decay} (fs)	τ_{rise} (fs)	Time shift (fs)
$Fe(CO)_5$	100 ± 5	⋯	⋯
$Fe(CO)_4$	105 ± 5	⋯	20 ± 5
$Fe(CO)_3$	115 ± 5	⋯	30 ± 5
$Fe(CO)_2$	150 ± 20	⋯	60 ± 15
Fe(CO)	230 ± 20	120 ± 20	⋯
Fe	490 ± 50	260 ± 20	⋯

In summary, the most important features observed in this two color pump–probe experiment are the following:

(i) Essentially the same decay times (≈100 fs) have been observed for the parent molecule and $Fe(CO)_n$, $n=2-4$ fragments with no detectable rise time.
(ii) $Fe(CO)_n$, $n=2-4$ transients are time shifted with respect to that of the parent molecule $Fe(CO)_5$ by increasing time differences.
(iii) Only the transients of the Fe(CO) and Fe fragments show rise times. The Fe(CO) rise time is on the order of the decay time observed for the parent molecule. The Fe rise time is very close to the decay time measured for Fe(CO).
(iv) Additionally, the Fe transient shows a decay time.

From the results summarized above, we conclude that the photodissociation of $Fe(CO)_5$ in the gas phase occurs on an ultrafast time scale (few hundreds of femtoseconds). This ultrafast time scale for the photodissociation process should exclude the possibility of statistical energy transfer within the molecule prior to fragmentation (IVR) or internal conversion, as it has been pointed out for the related $Mn_2(CO)_{10}$ molecule.[37] Nevertheless, the same group[71] reported for the $(CH_3)_2CO$ molecule the appearance of intermediate fragments with redistributed vibrational energy, whereas IVR was excluded for the primary photodissociation step. Within our model, the observation of the time shifts could be ascribed as the beginning of IVR.

In order to understand the nature of the dissociation mechanism, we first discuss the photodissociation reaction in which only one CO ligand leaves the complex, i.e., $Fe(CO)_5 \rightarrow Fe(CO)_4 + CO$. A mechanism for this reaction, originally proposed by Daniel *et al.*[10] and supported by *ab initio* calculations,[10] involves the lowest electronically excited state of $Fe(CO)_5$, the triplet $^3E'$, which is a dissociative LF state. This state correlates with the $^3B_2$ ground state of $Fe(CO)_4$. The ground state of $Fe(CO)_5$ is a singlet $^1A_1'$, and a direct optical excitation should promote the molecule to a singlet electronically excited state. Daniel *et al.* proposed that after a spin and symmetry-allowed optical excitation to the low lying $^1E'$ state, the $^3E'$ state, which is close in energy, is populated by intersystem crossing (ISC). The fragmentation proceeds along the metal–ligand reaction coordinate where it crosses to the electronic ground state of $Fe(CO)_4$ ($^3B_2$), resulting in a vibrationally excited species.

The possibility of a direct optical excitation to the $^3E'$ state was not completely ruled out by Daniel *et al.*[10] because, although the transition is not spin allowed, the forbiddenness could be removed or, at least, reduced due to spin–orbit coupling with a singlet excited state.

In the present experiments, the parent molecule is excited to a total energy of 50 000 cm^{-1} (see above). A higher energy, MLCT-type, singlet electronic state could be a good candidate for such an excitation, as it has been pointed out elsewhere.[49,50,55,56] A nonadiabatic crossing to a triplet state close in energy may, however, take a few picoseconds for this molecule, since the spin–orbit coupling is not very strong for the first row transition metal complexes.[67,68] Therefore, it is most likely that the dissociation of $Fe(CO)_5$ proceeds directly from the optically pumped singlet state up to some electronically excited singlet state of the products.

In this case, if we consider a value of 1.82 eV for the first dissociation energy of $Fe(CO)_5$,[23] the available energy after absorption of two photons of 400 nm would be 4.38 eV. If all the available energy is transformed into translation of the fragments, the upper bound for the fragments recoil velocity would be ≈ 0.06 Å fs^{-1}. As pointed out by Zewail and co-workers,[37] the measured time shift could be related with the time needed by the fragments to go away from their force field interaction. Therefore, in the present case, the observed time shift of 20 ± 5 fs corresponds to a separation between the center of mass of the $Fe(CO)_4$ and CO fragments of ≈ 1 Å from the equilibrium distance. For a one-dimensional repulsive potential $V(R)=E\ \exp[-(R-R_0)/L]$, the length parameter L is determined from the relationship between the time shift, the recoil velocity, and the total energy,[79] and in our particular case, we get $L\approx 0.2$ Å. This value indicates a strongly repulsive potential. If, in addition, a substantial part of the available energy is retained by the nascent $Fe(CO)_4$ molecule as rovibrational excitation, as has been pointed out elsewhere,[47,48] then L could be even less than 0.2 Å, making the potential surface even more repulsive.[37]

A further issue to discuss is whether the ultrafast dissociation of $Fe(CO)_5$ occurs *stepwise* or in a *concerted* way. The available energy for $Fe(CO)_5$ after absorption of two photons of 400 nm is, however, enough to break the five Fe–CO bonds (see Fig. 1), and, actually, we are observing ionization transients for the parent molecule and every fragment. On a first glance, the present experiments seem to indicate that the mechanism for the photodissociation of $Fe(CO)_5$ is compatible with a stepwise fragmentation, since all the fragments are observed. However, $Fe(CO)_5$ and the $Fe(CO)_n$, $n=2-4$ fragments show similar decay times ($\approx 100-150$ fs) and no detectable rise time. In addition, the transients of the fragments exhibit a time delay of several tens of femtosecond with respect to the parent molecule. The fact that we observe essentially the same decay time for the parent and the $Fe(CO)_n$, $n=2-4$ fragments suggests that these transients are determined by the dynamics of only one intermediate species.

In a previous work, we proposed a simple model to explain these observations.[40] The model is as follows: $Fe(CO)_5$ is excited to a state with a total energy of 50 000 cm^{-1}. This state will evolve in a structural rearrangement during the first 20 ± 5 fs [the time shift observed in the $Fe(CO)_4$ transient]. At this particular geometry of the $[Fe(CO)_5]^{\ddagger}$ complex, the system absorbs probe laser photons yielding parent ions which undergo fragmentation into the measured $Fe(CO)_4^+$. The evolution of the multidimensional $[Fe(CO)_5]^{\ddagger}$ complex continues until another configuration is reached after 30 ± 5 fs. This new geometry of the complex now favors the production of $Fe(CO)_5^+$ ions, which undergo fragmentation into the measured $Fe(CO)_3^+$. This is the origin of the $Fe(CO)_3$ transient. With a very similar interpretation, we can account for the observed $Fe(CO)_2$ transient. Within the model, the decay times of about 100 fs correspond to the dissociation time of $Fe(CO)_5$ into Fe(CO)+4CO. The measured transients for $Fe(CO)_n$, $n=2-4$ represent snapshots of the evolution of the multidimensional $[Fe(CO)_5]^{\ddagger}$ transition state toward the loss of four CO ligands yielding the Fe(CO) fragments. Figure 10 shows a pictorial representation of the model.

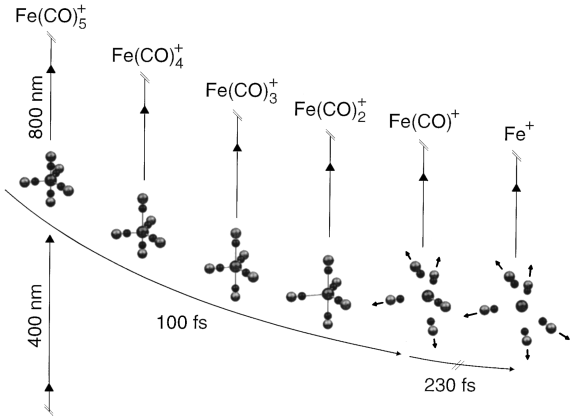

FIG. 10. Pictorial representation of the model proposed for the photodissociation mechanism of $Fe(CO)_5$. Electronically excited $Fe(CO)_5$ dissociates into Fe(CO)+4CO in about 100 fs. The ionization transient spectra measured for the $Fe(CO)_n$, $n=2-4$ fragments represent snapshots of the evolution of the multidimensional $[Fe(CO)_5]^{\ddagger}$ transition state on its way to dissociation. The last Fe–CO bond cleavage occurs on a longer time scale of 230 fs.

Furthermore, the ionization transient of Fe(CO) shows a rise time of 120 ± 20 fs. This rise time matches the $Fe(CO)_5$ dissociation time of 100–150 fs discussed above. In addition, a decay to a time independent signal level is observed with a time constant of 230 ± 20 fs. This is an indication that a distribution of different, maybe excited, Fe(CO) fragments are formed in the dissociation, and only part of the Fe(CO) fragments decay further. This decay time is close to the observed rise time of 260 ± 20 fs for the Fe fragment. The fit function for the Fe transient should consist of a time independent plateau and a difference of two exponentials, with one time constant corresponding to the decay of the $Fe(CO)_5$ parent molecule into Fe(CO) (about 100 fs) and a second one corresponding to the decay of Fe(CO). However, the contribution of the 100 fs rise can be neglected, especially after the convolution with the cross correlation. The analysis shows that the Fe transient could be fitted with a single-exponential rise.

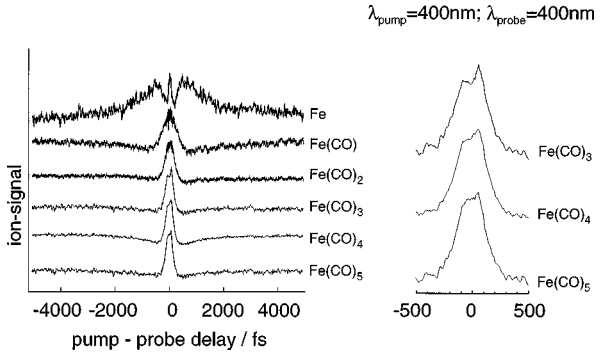

FIG. 11. One color (400 nm/400 nm) femtosecond transient ionization spectra of the parent molecule and of the fragments. The inset shows the expanded transients around time delay zero for the parent molecule and the $Fe(CO)_4$ and $Fe(CO)_3$ fragments.

Finally, we observe a long decay time of about 490 fs for the Fe fragments. Since Fe atoms cannot decay in such a short time, even if they are produced in highly excited states, this decay must be related to a process whose origin is in the precursors.

The idea of a concerted loss of ligands has been discussed by Jackson[7] for the related $Cr(CO)_6$. In that work, the fluorescence of electronically excited Cr atoms obtained after the photodissociation of $Cr(CO)_6$ produced by nanosecond laser excitation was measured in a gas cell at different pressures. The main conclusion of those experiments is when the excitation energy is high enough (corresponding to multiphoton absorption of the parent molecule) the dominant photodissociation mechanism is a concerted one. The parent molecule absorbs two, three or more photons coherently and a highly excited electronic state of the complex is prepared. This state will dissociate explosively, loosing several ligands simultaneously, in a time scale of just a single vibration. The dissociation process can be visualized then as a half-collision reaction, where the highly excited state of the parent molecule can cross onto multiple potential energy surfaces, each of them representing a different product metal containing fragment. To which extent this process occurs will depend on the available energy. Jackson[7] concluded that a sequential mechanism could gain more importance with respect to the concerted loss of ligands as the excitation energy decreases. Our results are in qualitative agreement with these conclusions. The $Fe(CO)_5$, electronically excited to 50 000 cm^{-1}, looses four CO ligands in just 100 fs. As typical vibrational periods of the Fe–CO bonds are between 80 and 100 fs,[15] this can be termed a concerted loss of the first four ligands. The subsequent dissociation of the formed Fe(CO) occurs on a longer time scale. After the explosive loss of up to four CO ligands following excitation of the parent molecule, the available energy is still large enough to initiate the rupture of the last Fe–CO bond, yielding Fe atoms.

B. 400/400 nm transients

Figure 11 shows the measured ionization transients for the parent molecule and every fragment ion obtained using the same color (400 nm) for both the pump and the probe lasers and laser intensities of about 10^{12} W cm^{-2}. Due to the fact that pump and probe wavelength as well as the intensities of both lasers are the same, the transients are symmetric with respect to time delay $\Delta t=0$. The parent molecule and $Fe(CO)_n$, $n=2-4$ fragment ion transients show a fast decay of about 100 fs. The width of the transients $Fe(CO)_n$, $n=2-5$ rises with the number of lost ligands and is always larger than the cross correlation of the laser pulses. For Fe(CO) and even more for Fe, the ionization transient is much wider and the decay is slower than for the larger fragments. Furthermore, all the transients show a double peak structure, and in the case of the Fe transient, we observe a narrow central peak whose FWHM is $\approx$85 fs. In addition to the fast decay, the parent molecule and the $Fe(CO)_n$, $n=1-4$ fragment ion transients show a very slow rise at longer delay times in the order of picoseconds.

These results are in qualitative agreement with the results obtained from the 400/800 nm pump–probe experiments. The similar decay times of about 100–150 fs for the $Fe(CO)_n$, $n=2-5$ and the fact that these transients show no rise are consistent with the two-color experiments. The double-peak structure and the broadening of the transients from large to small fragments fits the observation, made in the 400/800 nm pump–probe experiment, that these transients are time shifted with respect to $\Delta t=0$. The expected rise time of about 120 fs for the Fe(CO) transient cannot be resolved, but results in the clearly visible additional broadening of the 400/400 nm transient.

The observed one–color pump–probe ionization transients are strongly dependent on the intensity of the laser pulses. At the lowest laser intensities applied ($\approx 5\times10^{11}$ W cm^{-2}, not shown here), where practically no ions are observed from each laser alone, the ionization transients for the parent and all the fragments consisted of a symmetric peak around $\Delta t=0$ similar to that found in the Fe^+ transient of Fig. 11. As the laser intensity was increased, the different features observed in the transients of Fig. 11 started to appear. Most likely, these narrow peaks are produced via direct MPI of the parent molecule and following ionic fragmentation, the same process we have seen in the other femtosecond TOF mass spectra (see Sec. IV B).

These results are in qualitative agreement with the photodissociation mechanism proposed in the model, although a quantitative analysis of the transients in terms of decay times and time shifts is more difficult in this case due to the contribution to the transients of the symmetric ion signal around time delay $\Delta t=0$. These transients show the richness of the dynamics of this system when high pump–laser intensities (high in comparison to the 400/800 nm pump–probe experiment) are used. There are several different processes responsible for the observed dynamics, as can be seen most clearly from the Fe transient. From this transient, at least three different processes can be extracted: an immediate production of Fe^+ most likely via direct MPI of the parent and subsequent ionic fragmentation, a delayed rise in the Fe yield due to the dissociation of Fe(CO), and a delayed decay of about 490 fs. The slow rises on a picosecond time scale found in the larger fragments have not yet been fully understood.

VI. METASTABLE ION FRAGMENTATION

With a reflectron time-of-flight (RETOF) spectrometer we detect not only the ions formed in the interaction region, i.e., the space where the molecular beam and the laser overlap, but also ions (metastable ions with a lifetime of the order of the flight time) formed in different regions of the spectrometer. Basically, ions formed in the field-free drift region due to a metastable decay, reach the MCP detector according to their mass, in contrast to a linear TOF, where those so-called daughter ions hit the MCP detector simultaneously with their ionic precursors. The use of a RETOF in the energy correction mode provides a similar flight time for either the daughter ions and those ions with the same mass which have already been produced in the interaction region. When it is used in a partially correction mode, i.e., when the reflector potentials are detuned, the daughter ions have a different flight time compared to the ions with the same mass, formed in the interaction region. Therefore, by detuning the potentials, it is possible to observe the daughter ions.[82–84]

Figure 12 shows details of $Fe(CO)_5$ 400 nm RETOF spectra ($I \approx 10^{13}$ W cm^{-2}) for different reflector potentials. The mass peak indicated as $Fe(CO)_4^+$ belongs to $Fe(CO)_4^+$ ions, formed directly in the interaction region. By detuning the reflector potentials around the potentials where ideal energy correction is achieved, a peak crosses the $Fe(CO)_4^+$ peak. This crossing peak is also observed for the $Fe(CO)_3^+$ mass peak and with very low intensities even for the smaller fragments. In order to determine the precursor ions of these ions formed due to a metastable decay in the field free drift region, the reflectron time-of-flight spectrum was simulated with a computer. Figure 13 shows the flight times of the directly formed $Fe(CO)_{4,3}^+$ (squares) and the $Fe(CO)_{4,3}^+$ ions (circles), formed due to a metastable decay for different reflector potentials. The solid lines are fits of the times of flight. This fit was performed in the following manner. The time of flight was calculated for $Fe(CO)_5^+$ formed in the interaction region until it enters the field free drift region. At this point, a fragmentation with a mass loss of Δm was introduced. The four sets of data indicated in Fig. 12 were

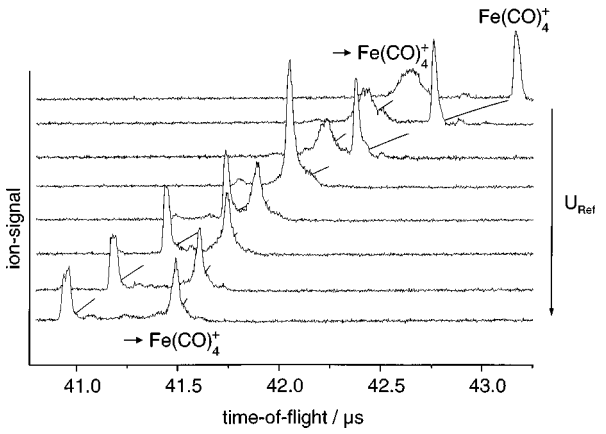

FIG. 12. Details of the reflectron TOF spectrum for $Fe(CO)_5$ around the $Fe(CO)_4^+$ mass peak for different reflector potentials taken at 400 nm ($I \approx 10^{13}$ W cm^{-2}). The peak denoted as $\rightarrow Fe(CO)_4^+$ results of the metastable decay of $Fe(CO)_5^+$ in the field free drift region.

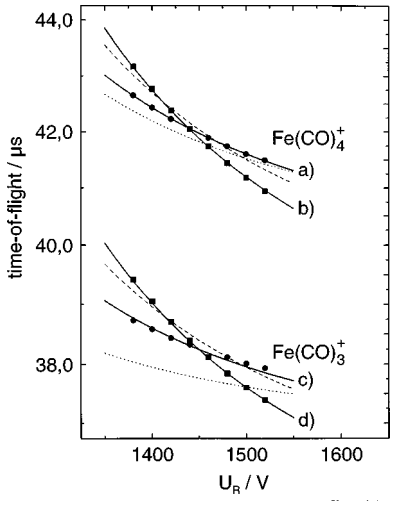

FIG. 13. Times of flight of the directly produced $Fe(CO)_4^+$ and $Fe(CO)_3^+$ ions (squares) and of those ions produced in the field free drift region due to a metastable decay (circles) for different reflector potentials: (a) Fit for the metastable produced $Fe(CO)_4^+$ (solid line): $Fe(CO)_5^+ \rightarrow Fe(CO)_4^+ + CO$. The case of a molecule losing mass 16 amu (dashed line) and mass 35 amu (dotted line) which fragments into $Fe(CO)_4^+$ is also included for comparison. (b) Fit for directly produced $Fe(CO)_4^+$ (solid line). (c) Fit for the metastable produced $Fe(CO)_3^+$ (solid line): $Fe(CO)_4^+ \rightarrow Fe(CO)_3^+ + CO$. The case of a molecule losing mass 16 amu (dashed line) and mass 35 amu (dotted line) which fragments into $Fe(CO)_3^+$ is also included for comparison. (d) Fit for directly produced $Fe(CO)_3^+$ (solid line).

fitted simultaneously. The precursors of the $Fe(CO)_4^+$ ions, formed in the field-free drift region, were calculated to be ions which lost a fragment with mass 30 ± 5 amu and 28 ± 5 for the $Fe(CO)_3^+$ ions. For comparison, a mass loss of 16 amu (dashed lines) and of 35 amu (dotted lines) was simulated. These fits show that the daughter ions were formed due to a metastable loss of one CO (28 amu) ligand. The time scale for this decay can be estimated to be in the range of 1–20 μs, the time the ions need to enter the field free drift region and the time of flight to the reflector.

This experiment shows, that in the case of $Fe(CO)_5$ after fs laser excitation with 400 nm radiation, we observe two completely different fragmentation mechanisms for different excitation energies. The time scales involved differ by several orders of magnitude and range from femtoseconds (two-photon excitation) to microseconds (multiphoton excitation).

VII. CONCLUSIONS

The ultrafast photodissociation dynamics of $Fe(CO)_5$ has been investigated in the gas phase using femtosecond laser pulses. Linear and reflectron time-of-flight (TOF) spectra were measured at different femtosecond laser wavelengths, pulse durations, and intensities, and the parent as well as all the fragments and even doubly charged species were observed. We find that the fragmentation pattern strongly depends on laser wavelength, pulse duration, and intensity. For ultrashort laser pulses the results are discussed in terms of a dissociative ionization mechanism.

One and two-color femtosecond pump–probe experiments have been performed to access the MLCT band with laser pulses at 400 and at 800 nm. Transient ionization spec-

tra have been measured for the parent molecule and every fragment. The time resolution of the experiments was high enough to resolve the dynamics of the photodissociation of $Fe(CO)_5$ and the loss of all CO ligands. From the analysis of the transients in terms of rise and decay times, a model for the photodissociation of $Fe(CO)_5$ is proposed. In this model, $Fe(CO)_5$ dissociates up to Fe(CO) in a concerted fashion, i.e., after absorption of two 400 nm photons, the parent molecule looses four CO ligands on the time scale of a vibrational period of the Fe–CO bond (≈ 100 fs). The measured $Fe(CO)_n$, $n=2-4$ ionization transients represent snapshots of the evolution of the multidimensional $[Fe(CO)_5]^{\ddagger}$ transition state on the way to the multiple-ligand loss. The excess energy is sufficient for a further dissociation of Fe(CO) into Fe and CO on a longer time scale.

Additionally, we reported on a completely different ionic fragmentation mechanism. A metastable decay of $Fe(CO)_n$, $n=5,4$ on a microsecond time scale is observed.

This work demonstrates the ultrafast dynamics of the photodissociation of $Fe(CO)_5$ in the gas phase and explains why nanosecond laser experiments failed to observe the $Fe(CO)_5^+$ and the corresponding CO containing fragment ions. Further investigations using other femtosecond laser wavelengths can give additional insight and may elucidate the important role the excitation energy plays in the photodissociation of this and other organometallic molecules.

ACKNOWLEDGMENTS

We are indebted to Dr. C. Daniel for helpful discussions and to A. Assion and V. Seyfried for their help in the experiments. L. B. gratefully acknowledges a research fellowship from the Alexander von Humboldt Stiftung of Germany. This work has been supported by the Deutsche Forschungsgemeinschaft through SFB 347. We would like to thank Professor H. Hotop from the University of Kaiserslautern for long time loan of a molecular beam apparatus. We would like to thank the referee for the very detailed and helpful comments and for the revision proposals he made on the manuscript.

[1] M. S. Wrighton, Chem. Rev. **74**, 401 (1974).
[2] G. L. Geoffrey and M. S. Wrighton, *Organometallic Photochemistry* (Academic, New York, 1979).
[3] M. S. Wrighton, D. S. Ginley, M. A. Schroeder, and D. L. Morse, Pure Appl. Chem. **41**, 671 (1975).
[4] Organic Synthesis via Metal Carbonyls, edited by I. Wender and P. Pino (Wiley, New York, 1977), Vols. 1 and 2.
[5] D. C. Bailey and S. H. Langer, Chem. Rev. **81**, 110 (1981).
[6] R. L. Jackson *et al.*, in *Laser Microfabrication*, edited by D. J. Ehrlich and J. Y. Tsao (Academic, New York, 1989), pp. 385–451.
[7] R. L. Jackson, Acc. Chem. Res. **25**, 581 (1992).
[8] D. Guenzburger, E. M. B. Saitovitch, M. A. De Paoli, and H. Manela, J. Chem. Phys. **80**, 735 (1984).
[9] C. W. Bauschlicher, Jr. and P. S. Bagus, J. Chem. Phys. **81**, 5889 (1984).
[10] C. Daniel, M. Bénard, A. Dedieu, R. Wiest, and A. Veillard, J. Phys. Chem. **88**, 4806 (1984).
[11] A. Veillard, A. Strich, C. Daniel, and P. E. M. Siegbahn, Chem. Phys. Lett. **141**, 329 (1987).
[12] M. Kotzian, N. Rösch, H. Schröder, and M. C. Zerner, J. Am. Chem. Soc. **111**, 7687 (1989).
[13] M. Ohno and W. von Niessen, J. Chem. Phys. **95**, 373 (1991).
[14] A. Marquez, C. Daniel, and J. F. Sanz, J. Phys. Chem. **96**, 121 (1992).
[15] V. Jonas and W. Thiel, J. Chem. Phys. **102**, 8474 (1995).
[16] L. A. Barnes, M. Rosi, and C. W. Bauschlicher, Jr., J. Chem. Phys. **94**, 2031 (1991).
[17] B. J. Persson, B. O. Roos, and K. Pierloot, J. Chem. Phys. **101**, 6810 (1994).
[18] J. Li, G. Schreckenbach, and T. Ziegler, J. Am. Chem. Soc. **117**, 486 (1995).
[19] A. W. Ehlers and G. Frenking, Organometallics **14**, 423 (1995).
[20] C. Adamo and F. Lelj, Chem. Phys. Lett. **246**, 463 (1995).
[21] A. Ricca and C. W. Bauschlicher, Jr., J. Phys. Chem. **98**, 12899 (1994).
[22] P. C. Engelking and W. C. Lineberger, J. Am. Chem. Soc. **101**, 5569 (1979).
[23] K. E. Lewis, D. M. Golden, and G. P. Smith, J. Am. Chem. Soc. **106**, 3905 (1984).
[24] G. Distefano, J. Res. Natl. Bur. Stand. Sect. A **74**, 233 (1970).
[25] L. F. Halle, P. B. Armentrout, and J. L. Beauchamp, Organometallics **1**, 963 (1982).
[26] K. Norwood, A. Ali, G. D. Flesch, and C. Y. Ng, J. Am. Chem. Soc. **112**, 7502 (1990).
[27] R. H. Schultz, K. C. Crellin, and P. B. Armentrout, J. Am. Chem. Soc. **113**, 8590 (1991).
[28] A. G. Joly and K. A. Nelson, Chem. Phys. **152**, 69 (1991).
[29] A. G. Joly and K. A. Nelson, J. Phys. Chem. **93**, 2876 (1989).
[30] P. A. Anfinrud, C.-H. Han, T. Lian, and R. M. Hochstrasser, J. Phys. Chem. **95**, 574 (1991).
[31] T. P. Dougherty and E. J. Heilweil, Chem. Phys. Lett. **227**, 19 (1994).
[32] A. Waldman, S. Ruhman, S. Shaik, and G. N. Sastry, Chem. Phys. Lett. **230**, 110 (1994).
[33] N. J. Tro, J. C. King, and C. B. Harris, Inorg. Chim. Acta **229**, 469 (1995).
[34] C. J. Arnold, T.-Q. Ye, R. N. Perutz, R. E. Hester, and J. N. Moore, Chem. Phys. Lett. **248**, 464 (1996).
[35] M. W. George, T. P. Dougherty, and E. J. Heilweil, J. Phys. Chem. **100**, 201 (1996).
[36] S. A. Angel, P. A. Hansen, E. J. Heilweil, and J. C. Stephenson, in *Ultrafast Phenomena VII*, edited by C. B. Harris, E. P. Ippen, G. A. Mourou, and A. H. Zewail, Springer Series in Chemical Physics Volume 53 (Springer-Verlag, Berlin, 1990), p. 480.
[37] S. K. Kim, S. Pedersen, and A. H. Zewail, Chem. Phys. Lett. **233**, 500 (1995).
[38] T. Lian, S. E. Bromberg, M. C. Asplund, H. Yang, and C. B. Harris, J. Phys. Chem. **100**, 11994 (1996).
[39] R. L. Whetten, K.-J. Fu, and E. R. Grant, J. Chem. Phys. **79**, 4899 (1983).
[40] L. Bañares, T. Baumert, M. Bergt, B. Kiefer, and G. Gerber, Chem. Phys. Lett. **267**, 141 (1997).
[41] M. Dartiguenave, Y. Dartiguenave, and H. B. Gray, Bull. Soc. Chim. Fr. 4223 (1969).
[42] C. E. Moore, Natl. Stand. Ref. Data Ser. (U.S. Natl. Bur. Stand.) **34**, (1970).
[43] Z. Karny, R. Naaman, and R. N. Zare, Chem. Phys. Lett. **59**, 33 (1978).
[44] D. W. Trainor and S. A. Mani, J. Chem. Phys. **68**, 5481 (1978).
[45] M. A. Duncan, T. G. Dietz, and R. E. Smalley, Chem. Phys. **44**, 415 (1979).
[46] P. C. Engelking, Chem. Phys. Lett. **74**, 207 (1980).
[47] J. T. Yardley, B. Gitlin, G. Nathanson, and A. M. Rosan, J. Chem. Phys. **74**, 370 (1981).
[48] G. Nathanson, B. Gitlin, A. M. Rosan, and J. T. Yardley, J. Chem. Phys. **74**, 361 (1981).
[49] A. J. Ouderkirk and E. Weitz, J. Chem. Phys. **79**, 1089 (1983).
[50] T. A. Seder, A. J. Ouderkirk, and E. Weitz, J. Chem. Phys. **85**, 1977 (1986).
[51] M. Poliakoff and J. J. Turner, J. Chem. Soc. Dalton Trans. 1351 (1973).
[52] M. Poliakoff and J. J. Turner, J. Chem. Soc. Dalton Trans. 2276 (1974).
[53] M. Poliakoff, J. Chem. Soc. Dalton Trans. 210 (1974).
[54] J. J. Turner, J. K. Burdett, R. N. Perutz, and M. Poliakoff, Pure Appl. Chem. **49**, 271 (1977).
[55] I. M. Waller, H. F. Davis, and J. W. Hepburn, J. Phys. Chem. **91**, 506 (1987).
[56] I. M. Waller and J. W. Hepburn, J. Chem. Phys. **88**, 6658 (1988).
[57] U. Ray, S. L. Brandow, G. Bandukwalla, B. K. Venkataraman, Z. Zhang, and M. Vernon, J. Chem. Phys. **89**, 4092 (1988).
[58] B. K. Venkataraman, G. Bandukwalla, Z. Zhang, and M. Vernon, J. Chem. Phys. **90**, 5510 (1989).
[59] J. J. BelBruno, P. H. Kobsa, R. T. Carl, and R. P. Hughes, J. Phys. Chem. **91**, 6168 (1987).
[60] Y. Nagano, Y. Achiba, and K. Kimura, J. Chem. Phys. **84**, 1063 (1986).

[61] S. Niles, D. A. Prinslow, C. A. Wight, and P. B. Armentrout, J. Chem. Phys. **93**, 6186 (1990).
[62] S. A. Mitchell and P. A. Hackett, J. Chem. Phys. **93**, 7813 (1990).
[63] K. Lee, J. S. Goo, and J. K. Ku, Chem. Phys. Lett. **244**, 213 (1995).
[64] K. Lee, H. S. Yoo, and J. K. Ku, Chem. Phys. Lett. **262**, 610 (1996).
[65] J. Manz, B. Reischl, T. Schröder, F. Seyl, and B. Warmuth, Chem. Phys. Lett. **198**, 483 (1992).
[66] C. Daniel, M. C. Heitz, L. Lehr, T. Schröder, and B. Warmuth, Int. J. Quantum Chem. **52**, 71 (1994).
[67] C. Daniel, M. C. Heitz, J. Manz, and C. Ribbing, J. Chem. Phys. **102**, 905 (1995).
[68] M.-C. Heitz, C. Ribbing, and C. Daniel, J. Chem. Phys. **106**, 1421 (1997).
[69] K. A. Trentelmann, S. H. Kable, D. B. Moss, and P. L. Houston, J. Chem. Phys. **91**, 7498 (1989).
[70] C. E. M. Strauss and P. L. Houston, J. Phys. Chem. **94**, 8751 (1990).
[71] S. K. Kim, S. Pedersen, and A. H. Zewail, J. Chem. Phys. **103**, 477 (1995).
[72] T. Baumert and G. Gerber, Adv. At., Mol., Opt. Phys. **35**, 163 (1995).
[73] K. F. Willey, C. L. Brummel, and N. Winograd, Chem. Phys. Lett. **267**, 359 (1997).
[74] T. Baumert, R. Thalweiser, V. Weiss, and G. Gerber, in *Femtosecond Chemistry*, edited by J. Manz and L. Wöste (VCH, Weinheim, 1995), pp. 397–432.
[75] T. Baumert and G. Gerber, Phys. Scr. **T72**, 53 (1997).
[76] C. Weickhardt, F. Moritz, and J. Grotemeyer, Eur. Mass Spectrom. **2**, 151 (1996).
[77] C. Grun, C. Weickhardt, and J. Grotemeyer, Eur. Mass Spectrom. **2**, 197 (1996).
[78] In Ref. 74.
[79] A. H. Zewail, *Ultrafast Dynamics of the Chemical Bond* (World Scientific, Singapore, 1994), and references therein.
[80] A. Assion, M. Geisler, J. Helbing, V. Seyfried, and T. Baumert, Phys. Rev. A **54**, R4605 (1996).
[81] T. Baumert, J. Helbing, and G. Gerber, in *Advances in Chemical Physics—Photochemistry: Chemical Reactions and their Control on the Femtosecond Time Scale*, edited by I. Prigogine and S. Rice (Wiley, New York, 1997), Vol. 101, pp. 47–77.
[82] M. Y. M. Lyktey, P. Xia, and J. F. Garvey, Chem. Phys. Lett. **238**, 54 (1995).
[83] O. Echt, P. D. Dao, S. Morgan, and A. W. Castleman, Jr., J. Chem. Phys. **82**, 4076 (1985).
[84] S. Morgan and A. W. Castleman, Jr., J. Phys. Chem. **93**, 4544 (1989).